

# Investigation Of SWIPT NOMA Over Rayleigh Fading

Dr.Sumit Gupta<sup>a\*</sup>, Sneha Maram<sup>2</sup>, Laxmi Priya Nakka<sup>b</sup>, Himaja Veeragoni<sup>b</sup>, Hrushikeah.panduga<sup>b</sup>, Arpita baronia<sup>c</sup>

*Dept of ECE Assistant professor , SR University WARANGAL, INDIA<sup>a</sup>  
Dept.of ECE,SR Engineering College,Warangal,India<sup>b</sup>  
Dept of CSE Assistant professor, VIT,Bhopal<sup>c</sup>  
Sumitmanit25@gmail.com*

## Abstract

Non-orthogonal multiple access (NOMA), which may be utilized to increase spectral efficiency in fifth-generation (5G) networks, has recently generated a lot of attention. In this part, we will examine how the concepts of simultaneous wireless power transfer (SWIPT) and non-orthogonal multiple access (NOMA) can be coupled to create a unique wireless energy harvesting multiple access protocol that is both energy- and spectrum-efficient. The signal is amplified for the NOMA users farther away who are experiencing worse channel conditions by using the NOMA users closer to the source as relays. The chapter considers how SWIPT might be used in NOMA, particularly when it's done by people who are close to the access points. We propose three opportunistic user selection methods for NOMA implementation: nearest near user and farthest far user (NNFF) selection, closest near user and nearest far user (NNNF), and random near user and random far user (RNRF).

Keywords: fifth-generation network, NOMA, SWIPT, Energy Harvesting.

## Nomenclature

$T$	Transmit Power
$a_n$	Fraction of power allocated to near user
$a_f$	Fraction of power allocated to far user
$x_n$	Signal intended for near user
$x_f$	Signal intended for far user
$h_{sn}$	Rayleigh fading coefficient between the BS and near user with zero mean and variance $= d_{sn}^{-\eta}$
$d_{sn}$	Distance between BS and near user
$\eta$	Path loss exponent
$w_n$	AWGN With zero mean and variance $= \sigma^2$

## 1. Introduction

There has been a considerable increase in smart devices, new technology, and contemporary applications, which has led to the wireless communication industry seeing tremendous growth. The maximum budget for transmit power, minimum data rate, and minimal gathered energy per terminal restrictions [19]. The performance of a system is measured using two different metrics: energy efficiency (EE) and spectral efficiency (SE) [1]. In order to ensure its viability and meet its needs, the future generation of 6G will unavoidably require the efficient use of energy [2]. The relationship between bandwidth efficiency (BE) and energy efficiency (EE) is also investigated [6]. The availability of bandwidth (BW) is used to calculated by SE. The near NOMA users operate as energy harvesting relays for far NOMA users in the co-operative SWIPT NOMA protocol [4]. A timeline of the various efforts made to bring 6G into existence. major technology advances to meet connection objectives within 6G [7]. Green

\* Dr.Sumit Gupta  
E-mail address: sumitmanit25@gmail.com

NOMA is used to pinpoint energy-efficient NOMA plans. In a perfect world, the energy needed for communication is sustainably handled [18]. The availability of bandwidth (BW) is used to calculated by SE. The simultaneous wireless information and power transmission (SWIPT) with cooperative hybrid-NOMA (H-NOMA) in terahertz (THz) is an improved two-user pairing technique that considers SIC imperfection [12]. Future generations will be significantly impacted by terahertz (THz) communication. The problematic shortfalls that THz communications face because of THz features are thought to be overcome by cooperative simultaneous wireless information and power transmission (THz-NOMA) [9]. Users with better channel conditions obtain less power from NOMA, and by using successive interference cancellation, these users can decode their own information [5]. The unknown electromagnetic (EM) gap (0.1–10 THz) between EM and optical bands is represented by THz. A new cooperation strategy allows a two-user cooperative non-orthogonal multiple access network to directly connect with nearby users [16]. Electronic, photonic, and plasmonic technologies are anticipated to be used in the production of THz transmitters and receivers. By comparing the procedures used at the transmitter, the state-of-the-art NOMA systems are evaluated [17]. Investigations on the NOMA approach for 5G wireless communication have improved channel capacity while taking user fairness restrictions into account.

Because of needs for the Internet of Everything (IoE), fully connected systems are now necessary. 5G systems are constrained, making it unable to add features or improve existing ones to meet these requirements to improve the overall performance of 6G wireless communications and reliability, as well as wireless connectivity, resource management, scalability, and user fairness. Using MIMO-NOMA technology and THz frequencies, we modified the existing wireless communication systems while evaluating the effectiveness and gains made. Modern non-orthogonal multiple access (NOMA) variations that use power and code domains as the foundation for interference reduction, resource allocation, and quality of service management in the 5G scenario [15].

The main contribution is a stable non-LOS (NLOS) line of THz communications to make up for the absence of THz coverage in wide areas or any other place where IRS cannot be deployed. A base station (Bs) of the cooperative system connects directly with a user who is close by, while a relay node (RN) assists the Bs in communicating with the user who is far away [11]. By comparing related recent research on performance analysis of cooperative PD-NOMA systems, we may examine current trends in PD-NOMA based cooperative networks [8]. By using THz, NOMA, MIMO, cooperative networking, and EH (SWIPT) methods, as well as enhancing SE, EE, and other metrics in compared to the state of the art, it is possible to create a system with low power consumption, complexity, and cost [20].

### 1.1. RF Energy Harvesting

In the academic literature, several methods for energy harvesting have been investigated [13,14]. Among them, radio frequency energy harvesting (RFEH) stands out as a popular technique for converting energy from the electromagnetic field into electrical energy (i.e., voltage and current). RFEH has great potential for powering low-power sensors and systems in body area networks because it enables wireless power transfer in various application scenarios [3]. Nevertheless, harvesting energy from RF sources presents a challenging task for designers and researchers since it requires expertise from both the electromagnetic field and electronic circuit domains. Therefore, designing a high-performance RF energy harvester necessitates knowledge from both domains. There are two types of energy harvesting:

#### 1.1.1. Energy Harvesting by Time Switching:

The system operates in a time-slot based manner. During the first portion of the time slot, the device collects electromagnetic energy from its environment. The succeeding segment of the time slot is utilized to transmit the harvested energy. In subsequent articles, we will delve into time-switching further. This write-up will showcase the application of the cooperative NOMA power-splitting technique.

#### 1.1.2. Energy Harvesting by Power Splitting:

The device divides the signal power received to generate energy and decode data. The simultaneous implementation of energy harvesting and information decoding is possible with power splitting as opposed to time switching, which necessitates different time slots for both activities. SWIPT, or Simultaneous Wireless Information and Power Transfer, is another name for this technique.

## 2. Background

The most well-known candidate for creating 6G systems is hence nonorthogonal multiple access in the power domain (NOMA). Multi-input, multi-output (MIMO)-NOMA. The NOMA method improves channel capacity primarily defined by BW by superimposing numerous signals at the transmitter (Tx) and filtering them at the receiver (Rx) using successive interference cancellation (SIC) methods. By giving various power coefficients to users based on their channel conditions, NOMA multiplexing is accomplished. Line of sight (LOS) is the main transmission path, and clustering or grouping the serviced users is essential for improving SE and improving NOMA-based THz transmission. Implementing energy harvesting (EH) with cooperative NOMA takes use of cooperative networking's many advantages, including improved reliability and capacity as well as a greater coverage area.

## 3. Related Work

The major advantages of cooperative networking have already been studied using a range of cases and circumstances, and the disadvantages of using this method have also been addressed. The shortcomings, limitations, and poor performance of using those technologies were all carefully examined. The intelligent reflecting surface (IRS) must outperform the use of relaying in terms of complexity, energy, and cost in order to improve source-to-destination transmission in particular circumstances of interrupted communication paths, as demonstrated in Figure. The overall conclusion of this investigation claimed that a superior data rate is required to exceed the decode-forward (DF) relay regarding transmit power minimization and energy efficiency (EE) maximization when comparing IRS to the earlier DF relay. Additionally, IRS needs additional hardware.

Matching transmission beams for time-based steering, interference control, and EE degradation are some of the challenges in building and installing IRS to enable 6G communication networks. when deploying IRS, the effects of the actual coverage area, the hardware, the system components, and added maintenance/cost for wireless communications. Failures in aggregate or proportion are brought on by atmospheric factors.

### 3.1. Cooperative SWIPT NOMA Network

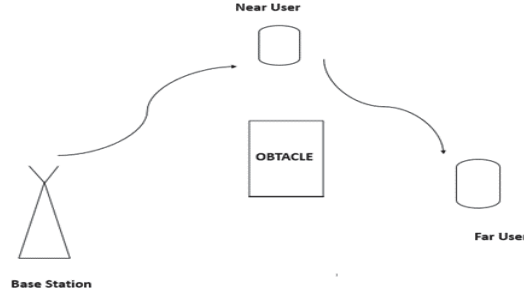


Fig. 1. Network Model of Cooperative SWIPT NOMA

In this scenario, we consider a downlink transmission model, where the base station (BS) utilizes NOMA to transmit messages simultaneously to both nearby and distant users. Unfortunately, an obstacle between the BS and the far user results in significant shadowing, rendering the signal undetectable to the distant user.

Conversely, the nearby user experiences clear communication with the BS. According to NOMA principles, the near user decodes the data intended for the far user first, and then utilizes successive interference cancellation (SIC) to decode its own data. The nearby user copies the far user's information, serving as a decode-and-forward relay to aid the distant user.

However, the challenge arises from the nearby user's lack of sufficient power to transmit data to the far user. To address this issue, the nearby user employs a power-splitting method of energy harvesting, specifically SWIPT, to accumulate additional power.

The entire communication process can be divided into two time slots. During the first time slot, the BS transmits data to the nearby user, who utilizes power-splitting to harvest a portion of the received signal power and utilizes the remainder for information decoding. In the second time slot, the nearby user employs the collected energy to transmit data to the far user.

### 3.2. Signal model of SWIPT NOMA

#### 3.2.1. Time Slot-1

In the first time slot, the BS transmits the NOMA signal, which is provided by

$$x = \sqrt{T} (\sqrt{a_n} x_n + \sqrt{a_f} x_f) \quad (1)$$

The remote user is unable to receive this signal because of severe shadowing. The signal that the near user receives is provided by,

$$y_n = \sqrt{T} (\sqrt{a_n} x_n + \sqrt{a_f} x_f) h_{sn} + w_n \quad (2)$$

The nearby user extracts a little amount of power from  $y_n$ , Let's use to represent this fraction  $\psi$ . This is known as the energy harvesting coefficient. The amount of power left over is  $(1 - \psi)$  the portion that can be used to decode information.

Therefore, the signal that can be used for information decoding after energy harvesting is,

$$y_D = (\sqrt{1 - \psi}) y_n + w_{eh} = (\sqrt{1 - \psi}) \sqrt{T} (\sqrt{a_n} x_n + \sqrt{a_f} x_f) + (\sqrt{1 - \psi}) w_n + w_{eh} \quad (3)$$

Where  $w_{eh}$  (with a zero mean and a variance of  $\sigma^2$ ) is the thermal noise produced by the energy harvesting electronics.

For the sake of simplicity, let's assume that the energy obtained via  $w_n$  is insignificant, which results in the following expression for  $y_D$ .

$$y_D = (\sqrt{1 - \psi}) \sqrt{T} (\sqrt{a_n} x_n + \sqrt{a_f} x_f) + w_{eh}$$

The nearby user initially carries out direct decoding of  $x_f$  from  $y_D$ . The feasible rate for the nearby user to decode data from the distant user is provided by,

$$R_{nf} = \frac{1}{2} \log_2 \left( 1 + \frac{T(1-\psi)a_f |h_{sn}|^2}{T(1-\psi)a_n |h_{sn}|^2 + \sigma^2} \right) \quad (5)$$

The rate at which a nearby user can successfully decode its own information after SIC is,

$$R_n = \frac{1}{2} \log_2 \left( 1 + \frac{T(1-\psi)a_n |h_{sn}|^2}{\sigma^2} \right) \quad (6)$$

$\psi$  is the fraction of power harvested in the time slot 1, the amount of power harvested is given by,

$$T_H = T |h_{sn}|^2 \zeta \psi \quad (7)$$

$\zeta$  is given by power harvesting efficiency of the circuitry.

### 3.2.2. Time slot-2

Using the power harvesting in the prior slot, the near user transmits the data intended for the far user  $p_H$ . The signal sent by the nearby user is,  $\sqrt{T_H} \bar{x}_f$ . The signal at the far user is,

$$y_f = \sqrt{T_H} \bar{x}_f h_{nf} + w_f \quad (8)$$

$h_{nf}$ , Rayleigh fading channel coefficient between near user and far user. The possible rate for a far user is,

$$R_f = \frac{1}{2} \log_2 \left( 1 + \frac{T_H |h_{sn}|^2}{\sigma^2} \right) \quad (9)$$

### 3.3. Optimize the power splitting coefficient

Now we will develop an expression in this part to get the ideal value of  $\psi$ . In the first time slot, the near user must successfully decode the data from the far user. The proper information can then be relayed in the subsequent time period. Let's create a constraint to verify this condition.

$$R_{nf} > R_f^* \quad (10)$$

$R_f^*$  is far user target data rate. The achievable rate at the near user must be higher than the far user's target rate in order to decode the data.

Let's substitute the expression of  $R_{nf}$  in the above condition and solve for  $\psi$

$$\frac{1}{2} \log_2 \left( 1 + \frac{T(1-\psi)a_f |h_{sn}|^2}{T(1-\psi)a_n |h_{sn}|^2 + \sigma^2} \right) > R_f^* \quad (11)$$

$$\log_2 \left( 1 + \frac{T(1-\psi)a_f |h_{sn}|^2}{T(1-\psi)a_n |h_{sn}|^2 + \sigma^2} \right) > 2R_f^* \quad (12)$$

$$1 + \frac{T(1-\psi)a_f |h_{sn}|^2}{T(1-\psi)a_n |h_{sn}|^2 + \sigma^2} > 2^{2R_f^*} \quad (13)$$

$$\frac{T(1-\psi)a_f |h_{sn}|^2}{T(1-\psi)a_n |h_{sn}|^2 + \sigma^2} > 2^{2R_f^*} - 1 \quad (14)$$

Let's denote  $2^{2R_f^*} - 1$  by  $P_f$ . This is the target SINR for the far user.

$$\frac{T(1-\psi)a_f |h_{sn}|^2}{T(1-\psi)a_n |h_{sn}|^2 + \sigma^2} > P_f \quad (15)$$

$$T(1-\psi)a_f |h_{sn}|^2 > P_f T(1-\psi)a_n |h_{sn}|^2 + P_f \sigma^2 \quad (16)$$

$$T(1-\psi)a_f |h_{sn}|^2 - P_f T(1-\psi)a_n |h_{sn}|^2 > P_f \sigma^2 \quad (17)$$

$$T(1-\psi) |h_{sn}|^2 (a_f - P_f a_n) > P_f \sigma^2 \quad (18)$$

$$(1-\psi) > \frac{P_f \sigma^2}{T |h_{sn}|^2 (a_f - P_f a_n)} \quad (19)$$

$$\psi < 1 - \frac{P_f \sigma^2}{T |h_{sn}|^2 (a_f - P_f a_n)} \quad (20)$$

To ensure that  $\psi$  is less than the value given by RHS, let's modify the above equation as,

$$\psi = 1 - \frac{P_f \sigma^2}{T |h_{sn}|^2 (a_f - P_f a_n)} - \delta \quad (21)$$

$\delta$  is a very small number. This value of  $\psi$  ensures that enough power is available for information decoding in order to meet the far user's target rate.

#### 4. Result and Analysis

As show in figure 1, While the far user's rate rises, the near user's rate reaches saturation at about 1 bps/Hz. This saturation is achieved by energy harvesting. All of the remaining power is gathered once the near user has reached the distant user's data rate. The energy harvesting function limits the possible rate at the nearby user even if the transmit power is raised. The benefit of this situation is that the target rate of 1 bps/Hz for the near user is not exceeded. As a result, the nearby user does not experience many outages due to this rate saturation.

The amount of power gathered rises as transmit power rises. As a result, the data sent by far users in the second slot is transmitted with more power. As a result, the achievable rate for far users rises. The user who is far away has a greater average attainable rate, so he must have the lowest chance of an outage as mention in Figure 3.

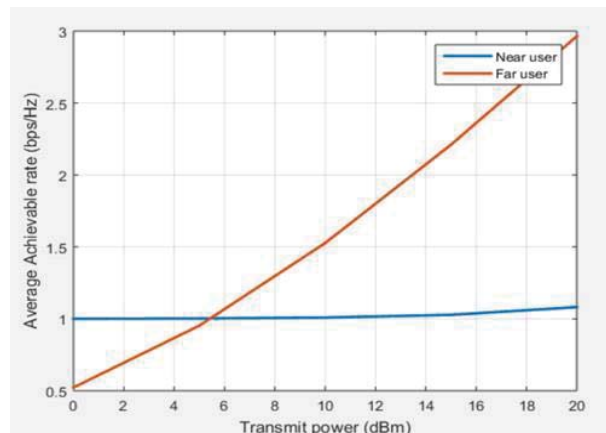


Fig. 2. Average achievable rates vs transmit power

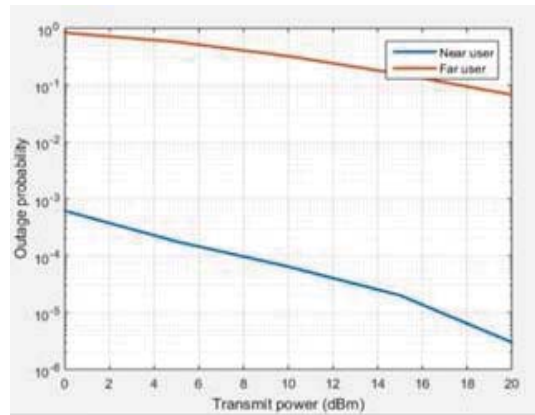


Fig. 3. outage performance of cooperative SWIPT NOMA

Despite having a higher attainable rate on average than the near user, the far user endures far more outages.

The far user's instantaneous achievable rate frequently falls below the goal rate value. How much higher the feasible rate is doesn't matter for outage calculations. We only keep track of instances in which the instantaneous rate deviates from the intended rate. For the remote user, this fall occurs more frequently as given in figure.4.

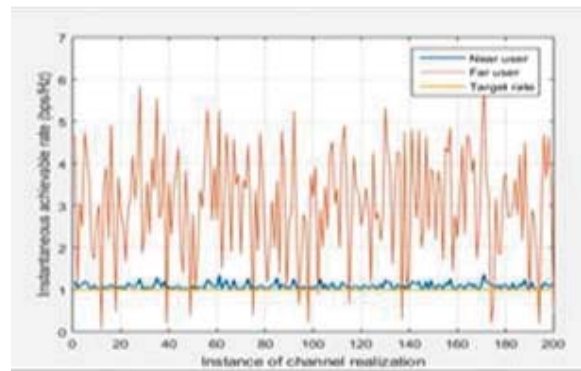


Fig. 4. instantaneous rates

## 5. Conclusion

The paper is concluded that, the far user experiences higher average achievable rate, but the no of counts that falls down the target rate explains the least outage performance. Although the near user has lesser achievable rate, but it is greater than the target rate most of the time. This explains better outage performance at near user.

## References

1. S. Han, T. Xie and C. -L. I, "Greener Physical Layer Technologies for 6G Mobile Communications," in IEEE Communications Magazine, vol. 59, no. 4, pp. 68-74, April 2021, doi: 10.1109/MCOM.001.2000484
2. G. Gür, "Expansive networks: Exploiting spectrum sharing for capacity boost and 6G vision," in Journal of Communications and Networks, vol. 22, no. 6, pp. 444-454, Dec. 2020, doi: 10.23919/JCN.2020.000037.
3. Introduction to RF Energy Harvesting Serdijn W.A., Mansano A.L.R., Stoopman M.(2014) *Wearable Sensors: Fundamentals, Implementation and Applications*, pp. 299-322.

4. Y. Liu, Z. Ding, M. ElKashlan and H. V. Poor, "Cooperative Non-orthogonal Multiple Access With Simultaneous Wireless Information and Power Transfer," in *IEEE Journal on Selected Areas in Communications*, vol. 34, no. 4, pp. 938-953, April 2016, doi: 10.1109/JSAC.2016.2549378.
5. Z. Ding, M. Peng and H. V. Poor, "Cooperative Non-Orthogonal Multiple Access in 5G Systems," in *IEEE Communications Letters*, vol. 19, no. 8, pp. 1462-1465, Aug. 2015, doi: 10.1109/LCOMM.2015.2441064.
6. Shankar R. Examination of a non-orthogonal multiple access scheme for next generation wireless networks. *The Journal of Defense Modeling and Simulation*. 2022;19(3):453-465. doi:10.1177/1548512920951277
7. I. F. Akyildiz, A. Kak and S. Nie, "6G and Beyond: The Future of Wireless Communications Systems," in *IEEE Access*, vol. 8, pp. 133995-134030, 2020, doi: 10.1109/ACCESS.2020.3010896.
8. Liaqat, M., Noordin, K.A., Abdul Latef, T. *et al.* Power-domain non orthogonal multiple access (PD-NOMA) in cooperative networks: an overview. *Wireless Netw* **26**, 181–203 (2020). <https://doi.org/10.1007/s11276-018-1807-z>
9. Oleiwi, H.W.; Al-Raweshidy, H. Cooperative SWIPT THz-NOMA/6G Performance Analysis. *Electronics* **2022**, *11*, 873. <https://doi.org/10.3390/electronics1106087>
10. Y. Liu, W. Yi, Z. Ding, X. Liu, O. A. Dobre and N. Al-Dhahir, "Developing NOMA to Next Generation Multiple Access: Future Vision and Research Opportunities," in *IEEE Wireless Communications*, vol. 29, no. 6, pp. 120-127, December 2022, doi: 10.1109/MWC.007.2100553.
11. O. Elkhartbotly, E. Maher, A. El-Mahdy and F. Dressler, "Optimal Power Allocation in Cooperative MIMO-NOMA with FD/HD Relaying in THz Communications," 2020 9th IFIP International Conference on Performance Evaluation and Modeling in Wireless Networks (PEMWN), Berlin, Germany, 2020, pp. 1-6, doi: 10.23919/PEMWN50727.2020.9293074.
12. H. W. Oleiwi, N. Saeed and H. S. Al-Raweshidy, "A Cooperative SWIPT-Hybrid-NOMA Pairing Scheme considering SIC imperfection for THz Communications," 2022 4th Global Power, Energy and Communication Conference (GPECOM), Nevsehir, Turkey, 2022, pp. 638-643, doi: 10.1109/GPECOM55404.2022.9815677.
13. X. Li, J. Li and L. Li, "Performance Analysis of Impaired SWIPT NOMA Relaying Networks Over Imperfect Weibull Channels," in *IEEE Systems Journal*, vol. 14, no. 1, pp. 669-672, March 2020, doi: 10.1109/JSYST.2019.2919654.
14. B. Makki, K. Chitti, A. Behravan and M. -S. Alouini, "A Survey of NOMA: Current Status and Open Research Challenges," in *IEEE Open Journal of the Communications Society*, vol. 1, pp. 179-189, 2020, doi: 10.1109/OJCOMS.2020.2969899.
15. I. Budhiraja et al., "A Systematic Review on NOMA Variants for 5G and Beyond," in *IEEE Access*, vol. 9, pp. 85573-85644, 2021, doi: 10.1109/ACCESS.2021.3081601.
16. G. Li and D. Mishra, "Cooperative NOMA Networks: User Cooperation or Relay Cooperation?," ICC 2020 - 2020 IEEE International Conference on Communications (ICC), Dublin, Ireland, 2020, pp. 1-6, doi: 10.1109/ICC40277.2020.9148973.
17. S. K. Zaidi, S. F. Hasan and X. Gui, "SWIPT-aided uplink in hybrid non-orthogonal multiple access," 2018 IEEE Wireless Communications and Networking Conference (WCNC), Barcelona, Spain, 2018, pp. 1-6, doi: 10.1109/WCNC.2018.8376963.
18. Y. Ye, Y. Li, D. Wang and G. Lu, "Power splitting protocol design for the cooperative NOMA with SWIPT," 2017 IEEE International Conference on Communications (ICC), Paris, France, 2017, pp. 1-5, doi: 10.1109/ICC.2017.7996751.
19. J. Tang et al., "Energy Efficiency Optimization for NOMA With SWIPT," in *IEEE Journal of Selected Topics in Signal Processing*, vol. 13, no. 3, pp. 452-466, June 2019, doi: 10.1109/JSTSP.2019.2898114.



20. S. Zargari, H. Ahmadinejad, B. Abolhassani and A. Falahati, "SWIPT-NOMA in Cell-Free Massive MIMO," 2020 28th Iranian Conference on Electrical Engineering (ICEE), Tabriz, Iran, 2020, pp. 1-6, doi: 10.1109/ICEE50131.2020.9260930.

### **Acknowledgement**

We thank SR Engineering College, Warangal, Telangana, and SR University, Warangal, Telangana for supporting us during this work.